Pergamon

J. Aerosol Sci., Vol. 25, No. 6, pp. 1213–1227, 1994

0021-8502/94 $7.00 + 0.00

0021-8502(94)E0036-W

THE MIXING OF ELECTRICALLY-CHARGED DROPLETS BETWEEN AND WITHIN ELECTROHYDRODYNAMIC FINE SPRAYS

PATRICK F. DUNN,* JEFFREY M. GRACE and STEPHEN R. SNARSKI

Particle Dynamics Laboratory, Hessert Center for Aerospace Research, Department of Aerospace & Mechanical Engineering, University of Notre Dame, Notre Dame, IN 46556, U.S.A.

(*First received* 19 *November* 1993; *and in final form* 17 *February* 1994)

Abstract—The results of experiments conducted to characterize droplet motion within electrohydrodynamic fine sprays are examined in the context of providing information on the mixing of electrically-charged droplets. Two cases are considered: one involving droplet mixing between two electrohydrodynamic fine sprays, and the other droplet mixing within a single electrohydrodynamic fine spray. The results collectively support that droplet mixing can be enhanced by relatively simple means, such as increasing the charge density of the spray, decreasing the separation distance between two sprays, or locally modifying the applied electric field within the spray.

INTRODUCTION

This paper examines the results of experiments conducted in our laboratory that provide information on droplet mixing in electrohydrodynamic (EHD) fine sprays. Herein, we consider two different aspects of electrically-charged droplet mixing: (1) that which occurs *between* two EHD sprays, a.k.a. *inter*-spray mixing, and (2) that which occurs *within* a single EHD spray, a.k.a. *intra*-spray mixing. More detailed information about our research on *inter*-spray mixing has been presented elsewhere (Dunn and Snarski, 1991; Snarski and Dunn, 1991). It is only summarized here. Our initial findings on *intra*-spray mixing were presented at a recent conference (Grace and Dunn, 1992) and are now presented in more detail in this paper.

Our research into both of these aspects of droplet mixing began by posing two practical questions: (1) can the electrically-charged droplets of two EHD sprays be mixed with one another to yield a single, combined spray, and (2) can droplet trajectories within a single EHD spray be controlled in a simple manner to produce a spatially uniform droplet size distribution and a narrower spray? These questions arose when considering how to electrostatically spray droplets into confined spaces, such as what occurs when two colors of electrostatically-sprayed paint are blended in flight before reaching a surface or when fuel is electrostatically sprayed into a car engine's cylinder through multiple ports.

Little consideration has been given to electrically-charged droplet mixing in the open literature. This is not surprising, because, up until only recently, the diagnostics required to accurately track the spatial evolution of droplet size, velocity and number concentration, and, hence, to quantitatively assess mixing, were not available. The only known cited observation related to electrically-charged droplet inter-spray mixing was given by Vonnegut and Neubauer (1952) in their study of the electrical atomization of water from glass capillaries. Based upon their observation of a "thin boundary of smoke-free air" between the resultant sprays, they concluded "the fact that both smokes are highly charged with the same sign prevents them from mixing." As shown later, this is not always the case; inter-spray mixing of droplets can occur despite their similar charge.

"Mixing" can have many meanings. The mixing of fluids can be considered to be the stretching and folding of fluid elements in space (which occurs by the *convection* of these elements), sometimes acting in concert with the *diffusion* of the elements themselves (Ottino,

* Author to whom correspondence should be addressed.

1989). The mixing of particles of different sizes in powders can be characterized by the spatial uniformity of the local concentration of each size (Nauman and Buffham, 1983), where the degree of mixing is quantified through a correlation coefficient based upon the concentration of a particle of specified size at one location versus that at another. A definition of EHD droplet mixing can be developed from the previous definitions. Mixing in EHD sprays can be defined as the convective transport of droplets into regions of the spray(s) where droplets would not be present in that size and/or number concentration under "normal"* circumstances. Based upon this definition, the degree of the mixing can be quantitatively assessed, e.g. by comparing the size distributions of the droplets at one location versus another location. In this sense, perfect mixing would imply the same size distribution everywhere.

In our studies of EHD droplet mixing, we have studied in detail only one particular type of EHD spray. We chose to investigate this particular spray because of the inherent polydispersity and spatial nonuniformity in its droplet population, making it very amenable to droplet mixing studies. This "EHD fine spray"† is produced readily in the laboratory by pumping an electrically conducting liquid at a constant volumetric flow rate through a capillary maintained at a high, positive potential difference with respect to an electrically grounded plate placed below the capillary. A polydisperse size distribution of droplets (diameters ~ 1–$50\ \mu m$) of moderate number concentration ($\sim 10^3$–10^4 droplets cm^{-3})

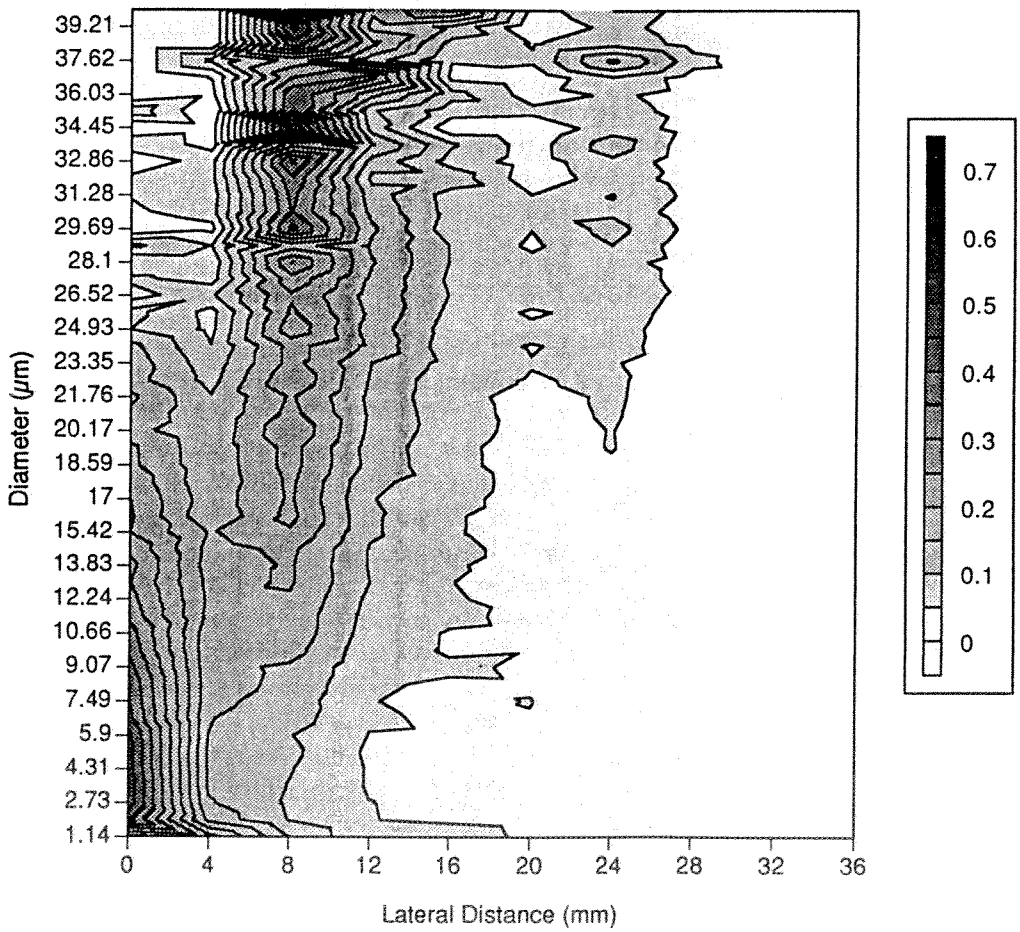

Fig. 1. Normalized droplet number concentrations for various droplet diameters as a function of the lateral distance from the axial centerline of a single EHD fine spray at 15 mm axial distance and a spray charge density of $\sim 300\ C\ m^{-3}$ (30 kV). The shaded scale indicates the normalized number concentration values, which equal the number concentration at that location divided by the value of 5000 droplets cm^{-3}.

*"Normal" refers to the unperturbed EHD fine spray, which is generated using a typical capillary-plate configuration.

† The "fine spray mode" is also referred to as the "rim emission mode", which is the limiting applied potential case of the "multiple cone-jet mode".

results, with droplet specific charges approximately one order of magnitude below their Rayleigh limit (~ 0.1 to 1 C kg^{-1}). The droplets are produced by the disruption of short, fine ligaments extending at various sites from the liquid meniscus, which is tightly bound to the capillary tip.* As shown by Grace (1993), a droplet's motion in the EHD fine spray in the region near its origin (the "near-field" region) is governed primarily by inertial, drag and electrical forces, and in the region away from its origin (the "far-field" region), primarily by drag and electrical forces. The extent of each region for a droplet depends upon its size. Droplets within the spray also are segregated spatially with respect to their size, with the smaller droplets residing more towards the center of the spray and the larger ones toward its periphery. A typical diameter-number concentration profile for this type of spray is displayed in Fig. 1.

EXPERIMENTAL APPROACH

A schematic of the typical apparatus used to generate and study the EHD fine spray is shown in Fig. 2. A stainless-steel hypodermic needle (27 gauge: 0.0406 cm o.d., 0.0216 cm i.d. and 1.9 cm length) serves as the capillary,† while an electrically grounded brass plate (60 cm $\times$ 60 cm) located 20 cm below the capillary tip serves as the electrical ground. A positive d.c. high voltage supply connected with the capillary generates electric field intensities at the capillary tip on the order of 10^6 V m^{-1}. The working fluid, ethanol (density = 789 kg m^{-3}, electrical resistivity = 50,000 Ωm, surface tension = 0.022 N m^{-1}), is pumped through the capillary at a constant mass flow rate of 5 mg s^{-1}. The resulting spray charge density‡

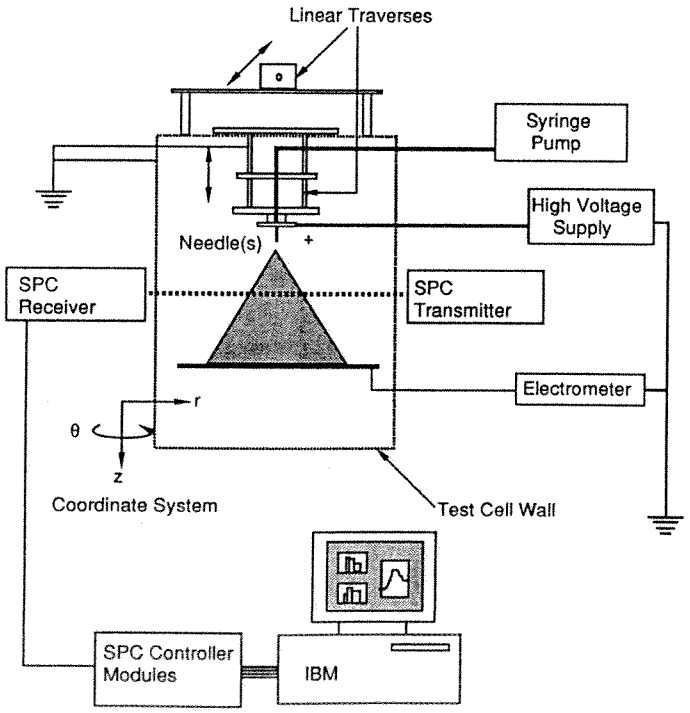

Fig. 2. Schematic of the EHD fine spray experimental apparatus. Only one needle and spray are shown here. For the inter-spray experiments, two parallel needles and sprays are present.

* For a detailed description of the experimental configuration and resulting droplet size and velocity distributions and number concentrations, see Grace (1993) for the single EHD fine spray, and Snarski (1988) for two, interacting EHD fine sprays.

†For the inter-spray experiments, two needles were used with their centerline axes aligned parallel to one another.

‡ The spray charge density is defined as the ratio of droplet current at the plate to volumetric flow rate. Its calculation optimistically assumes that there is no charge loss between the point of droplet origin and the plate. Actual charge losses for this configuration can be as high as approximately 30% (see Dunn and Snarski, 1992). The spray charge density differs from the space charge density, which is the total number of charges within the spray divided by the volume of the entire spray.

typically ranges from ~ 50 to 300 C m^{-3} for a variation in the applied voltage from ~ 15 to 30 kV. The primary diagnostic tool for these experiments is an *in situ*, laser-based Single-Particle Counter (SPC). We have used two individual SPCs based on different light-scattering principles: a Particle-Counter-Sizer Velocimeter (PCSV) (Holve and Annen, 1984) and a one-component Phase-Doppler-Particle Analyzer (PDPA) (Bachalo and Houser, 1984). Both of these systems provide measurements of the droplet diameter and number concentration, and droplet speed (the PCSV) or droplet velocity components and size-velocity component correlations (the PDPA). Because of the ranges of the droplet number concentrations and velocities encountered in the EHD fine spray, the average number of droplets in the measurement volume at any given time is on the order of 10^{-2}, which implies that coincidence errors in these measurements are negligible.

INTER-SPRAY DROPLET MIXING

The experimental results that provide information on droplet inter-spray mixing have been reported by Snarski (1988), Snarski and Dunn (1991) and Dunn and Snarski (1991). In those experiments, a PDPA system was used to probe the region of two interacting sprays generated from adjacent hypodermic needles (216 μm i.d.) located 38 cm above an electrical-

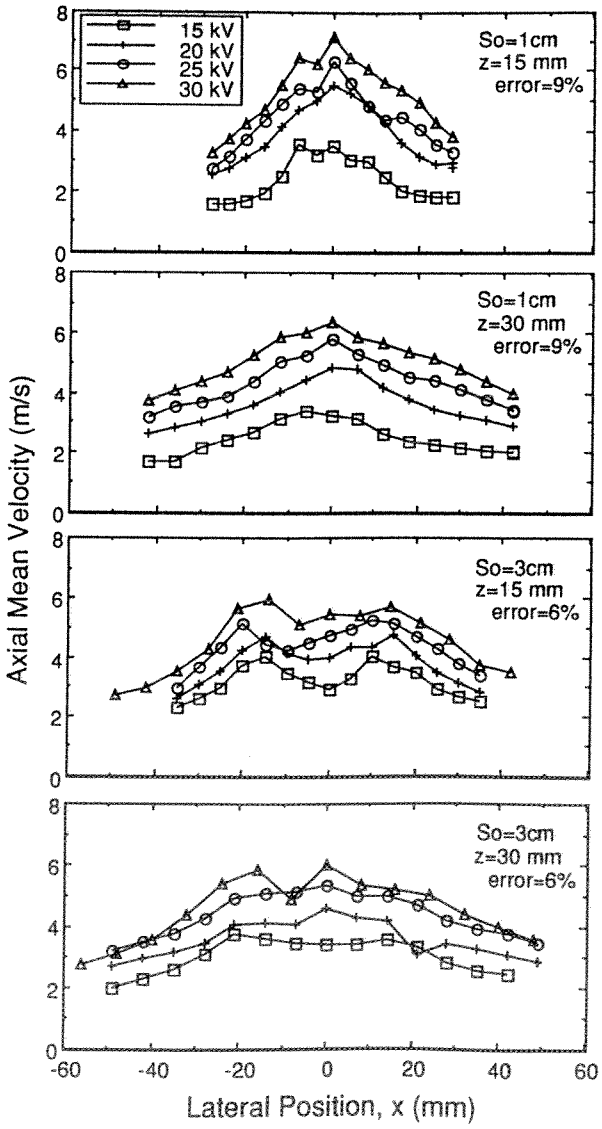

Fig. 3. Axial mean velocity profiles for 1 and 3 cm needle spacings, 15 and 30 mm axial locations and four applied voltages (from Snarski and Dunn, 1991).

ly grounded droplet-collection funnel. Data were acquired at two axial positions below the needles' tips (15 and 30 mm), for two inter-needle spacings (1 and 3 cm) and at four applied voltages (15, 20, 25 and 30 kV), corresponding to spray charge densities of approximately 60, 120, 180 and 280 C m^{-3}, respectively. By examining the velocity components and velocity-diameter correlations acquired in these experiments, the effects of spray charge density and needle spacing on inter-spray mixing can be deduced.

An enhanced spatial development of the combined spray as characterized by velocity profiles that approach one that is characteristic of a single spray can be viewed as indirect evidence of inter-spray droplet mixing. The axial and lateral mean droplet velocity component profiles across the lateral span of the interacting sprays for both needle spacings examined are presented in Figs 3 and 4. The axial mean velocity component profiles for the 1 cm needle spacing ($S_0 = 1$ cm) shown in Fig. 3 exhibit a magnitude that is maximum at the center and decreasing in the lateral direction. The lateral mean velocity component profiles, shown in Fig. 4, have a magnitude that is zero at the center and increasing in the lateral direction. These results for this spacing support that the two separate sprays have already merged and begun to develop into a single, uniform spray at the first axial position ($z = 15$ mm). By the second axial location ($z = 30$ mm), the spray is relatively spatially uniform, suggesting that inter-spray mixing has occurred.

The axial mean velocity component profiles for the 3 cm needle spacing ($S_0 = 3$ cm) and 15 mm axial location shown in Fig. 3 exhibit two local maxima located directly below the

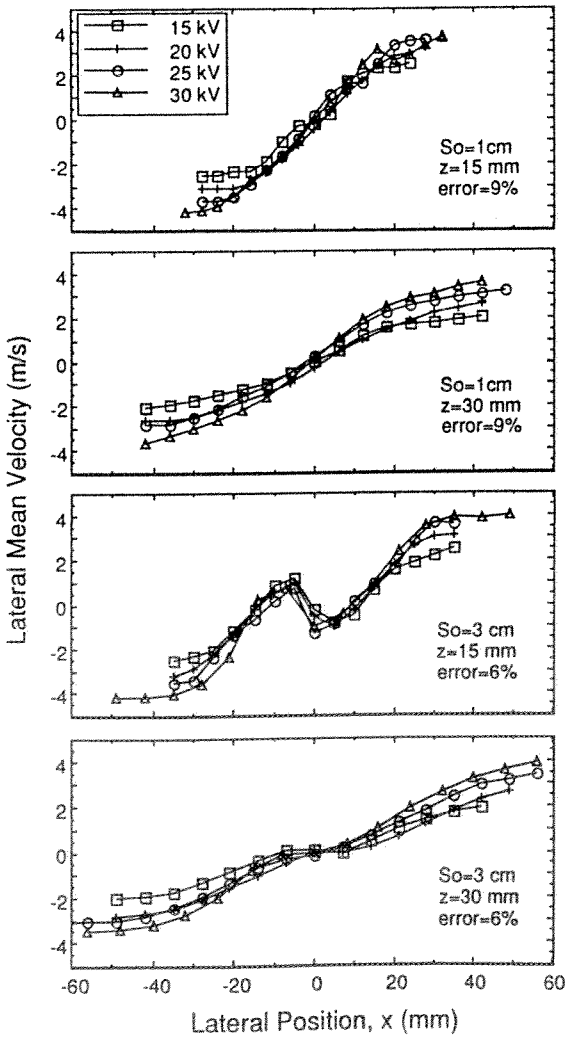

Fig. 4. Lateral mean velocity profiles for 1 and 3 cm needle spacings, 15 and 30 mm axial locations and four applied voltages (from Snarski and Dunn, 1991).

two needles' centerline axes. These maxima begin to lose their identity as the axial location is increased to 30 mm. The lateral mean velocity component profile at the 15 mm axial location for $S_0 = 3$ cm shown in Fig. 4 has a mean velocity component magnitude that is zero at the center. Moving laterally away from the center, this velocity component decreases, then increases, returning to a magnitude of approximately zero at the lateral positions of the two needles' centerline axes. This is the direct result of the inward lateral migration (i.e. mixing) of the droplets of the two sprays between the two needles' axial centerlines. At the 30 mm axial location, the lateral mean velocity component magnitude is approximately zero over a small center region and then increases in the lateral direction. The results for this 3 cm needle spacing indicate that the two separate sprays have just begun to merge at the second axial position, while at the first they are still somewhat distinct, individual sprays.

The effect of increasing applied voltage is also illustrated in Figs 3 and 4. An increase in applied voltage causes an increase in both the axial and lateral mean velocity components for both needle separations at all points within the spray. The increase in the axial mean velocity components results from a greater initial velocity imparted to the droplets because of their increased electrical mobility (which results from their increased charge and concomitant decreased diameter). The increase in the lateral mean velocity components results from the increased electrostatic repulsion between droplets, which is a consequence of the increase in droplet specific charge.

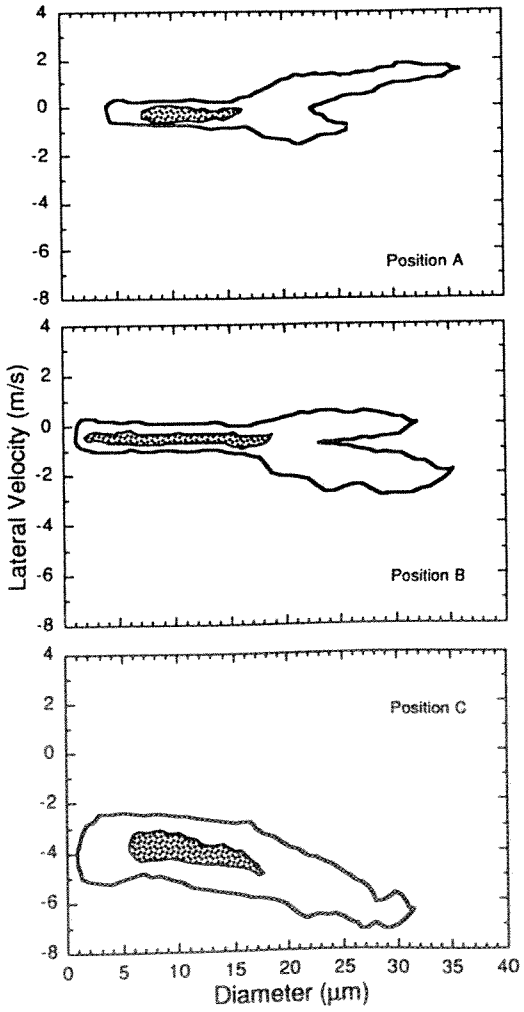

Fig. 5. Lateral velocity component–diameter correlation diagrams for positions A (the centerline between the two sprays), B (axially below one of the needles) and C (near the spray periphery), 1 cm needle spacing, 15 mm axial location and spray charge density of 278 C m^{-3} (from Dunn and Snarski, 1991).

Further evidence of inter-spray droplet mixing can be obtained by examining the correlations between the lateral velocity component and droplet diameter obtained for the 1 cm needle spacing at the 15 mm axial location, which is shown in Fig. 5. In this figure, the outer region(s) bounded by a solid line indicates where there were two or more occurrences of each possible velocity component-diameter point within that region. The inner, shaded region denotes where the majority of the droplet population resided, in which there were 10 or more occurrences of each possible velocity component-diameter point within that region. The correlation diagram for position A (at the centerline between the sprays) shows a bifurcation of the outer region at a droplet diameter of $\sim 22\ \mu m$, beyond which there are two distinct regions. This implies that there are two distinct lateral velocities for the same droplet diameter. This is evidence that the droplets from both sprays intermix at this centerline location, because these velocities are equal in magnitude but opposite in sign. On the contrary, if the droplets were repelled at the midplane between the two sprays, there would be a continuum of lateral velocity component values and not distinct regions for the same droplet diameter.* In the regions directly below the axis of either one of the two needles (position B), the correlation diagram reveals a decrease in the number of droplets from one population and an increase in the other. This is a direct consequence of moving laterally away from the spray of one of the needles and more into the other. Finally, the correlation diagram for a location near the periphery of either one of the sprays (position C) shows that only the droplets from one needle contribute to the velocity component distribution.

INTRA-SPRAY DROPLET MIXING

Grace (1993) and Grace and Dunn (1992) have reported the results of exploratory experiments related to intra-spray droplet mixing. In those experiments, both PDPA and PCSV systems were used to examine a single EHD fine spray generated from a hypodermic needle (27 gauge) located 20 cm above a large (60 cm × 60 cm) electrically grounded plate. Data were acquired at five axial positions below the needle's tip (5, 10, 20, 30 and 70 mm) at three applied voltages (15, 20 and 25 kV), corresponding to spray charge densities of approximately 70, 350 and 650 $C\ m^{-3}$, respectively. A laser light-sheet generated from a 5 W Ar-ion laser was used to illuminate either horizontal or vertical two-dimensional slices of the entire spray (~ 1 mm thick) at variable locations. This permitted visualization of individual droplet trajectories and their macro-scale organization into groups such as droplet "circulation cells".

One goal of these experiments was to identify a means of modifying two inherent characteristics of the EHD fine spray (droplet spatial segregation and spray lateral expansion) in order to achieve a more uniform size distribution throughout the spray and to confine its lateral expansion. This was accomplished by placing a small, electrically ground surface within the spray. The appropriate placement of this surface within the spray intensified the applied electric field at this location, forcing the charged droplets to converge on this point. Three experimental configurations were examined: two perturbed ones in which a small probe was placed within the spray, and a "normal" one in which no probe was present. The probe itself was made from a single, thin copper wire (0.5 mm o.d.) surrounded by a glass tube (2 mm o.d.), with only its wire tip (approximately 0.2 mm^2 surface area) directly exposed to the spray. This tip effectively served as an isolated, electrically grounded surface that perturbed the local electric field.† The probe tip was located 4 cm below the tip of the needle, either directly below the needle (the "on-axis" configuration) or displaced 2 cm laterally from it (the "off-axis" configuration).

* For the smaller droplet diameters ($< \sim 22\ \mu m$), the distinction between droplet inter-spray mixing or repulsion cannot be made because of inadequate resolution of the data in its present format.

† Liquid buildup on the outside surface of the glass tube also could influence the electric field in that region.

The "normal" configuration

The vertical light-sheet visualization of the EHD fine spray for this normal configuration is shown in Fig. 6, revealing an initial rapid, lateral dispersion of the droplets occurring in conjunction with a downward attraction toward the grounded plate. These droplets essentially follow electric field lines that arise from the combination of both internal (i.e. due to space charge) and external (i.e. due to the applied potential between the capillary and plate) electric fields (Grace, 1993). This composite field has a large radial component near the needle (because of the high droplet number concentration in that region) that decreases non-linearly toward a relatively negligible value at the plate.

Two-dimensional vector diagrams of the velocity field can be created for discrete sizes from the velocity component and size-velocity correlation information obtained using the PDPA system. As depicted in Fig. 7 for 20 μm diameter droplets, these diagrams quantitatively show the source-like spread of a typical EHD spray. In this figure, the magnitude of the velocities are shown in relation to the scale presented in the figure.* The PCSV-measured droplet speeds corroborate those speeds determined from PDPA velocity-component data; the speeds are high near the spray origin and lower farther towards the plate.

The "on-axis" configuration

This configuration produces a region along the axial centerline between the needle and probe that is relatively devoid of droplets. This is primarily because droplets emanating from their point of origin follow along the external electric field lines that spread laterally outward from the needle's tip and then converge laterally inward toward the probe's tip. This type of field curvature favors the formation of droplet "circulation cells". Over a short period of time, droplets accumulate within a cell until their number concentration is such that the space charge within the cell reaches a level that expels most of the droplets outward from it, effectively causing the cell to break down. This breakdown is periodic, with a frequency on the order of 1 Hz, and it promotes significant droplet interaction within that region of the spray.

Horizontal and vertical light-sheet visualizations of these cells are shown in Figs 8 and 9, respectively. The cells have distinct boundaries (see Fig. 8), being symmetrically spaced and

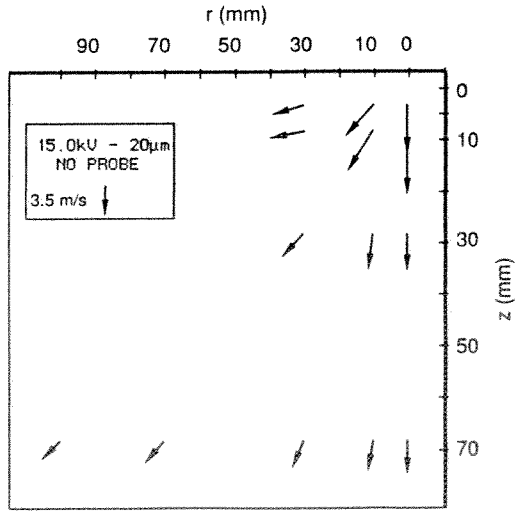

Fig. 7. Velocity vector diagram of 20 μm-diameter droplets in the EHD fine spray for the "normal" configuration at a spray charge density of 70 C m^{-3}. The tip of the needle is located at the coordinate (0,0).

* Note that only the velocities for the first one-third of the vertical dimension of the spray are displayed in the figure. Over this dimension, the magnitudes of the velocities decrease by a factor of approximately 1.5. Over the entire vertical dimension of the spray, they decrease by a factor of approximately 2.5.

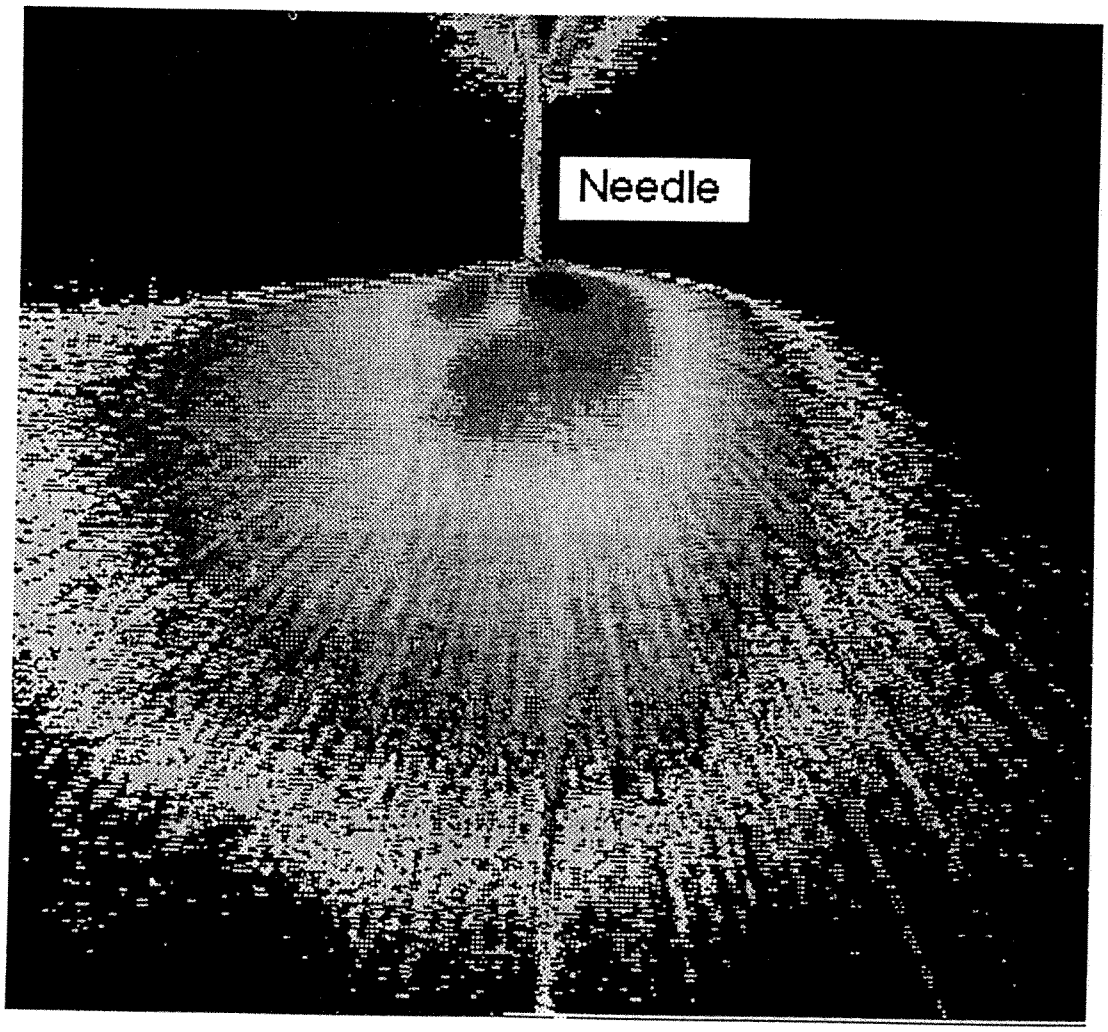

Fig. 6. Vertical light-sheet visualization of approximately a 10 cm × 10 cm cross-sectional area of the EHD fine spray for the "normal" configuration at a spray charge density of 70 $C\,m^{-3}$.

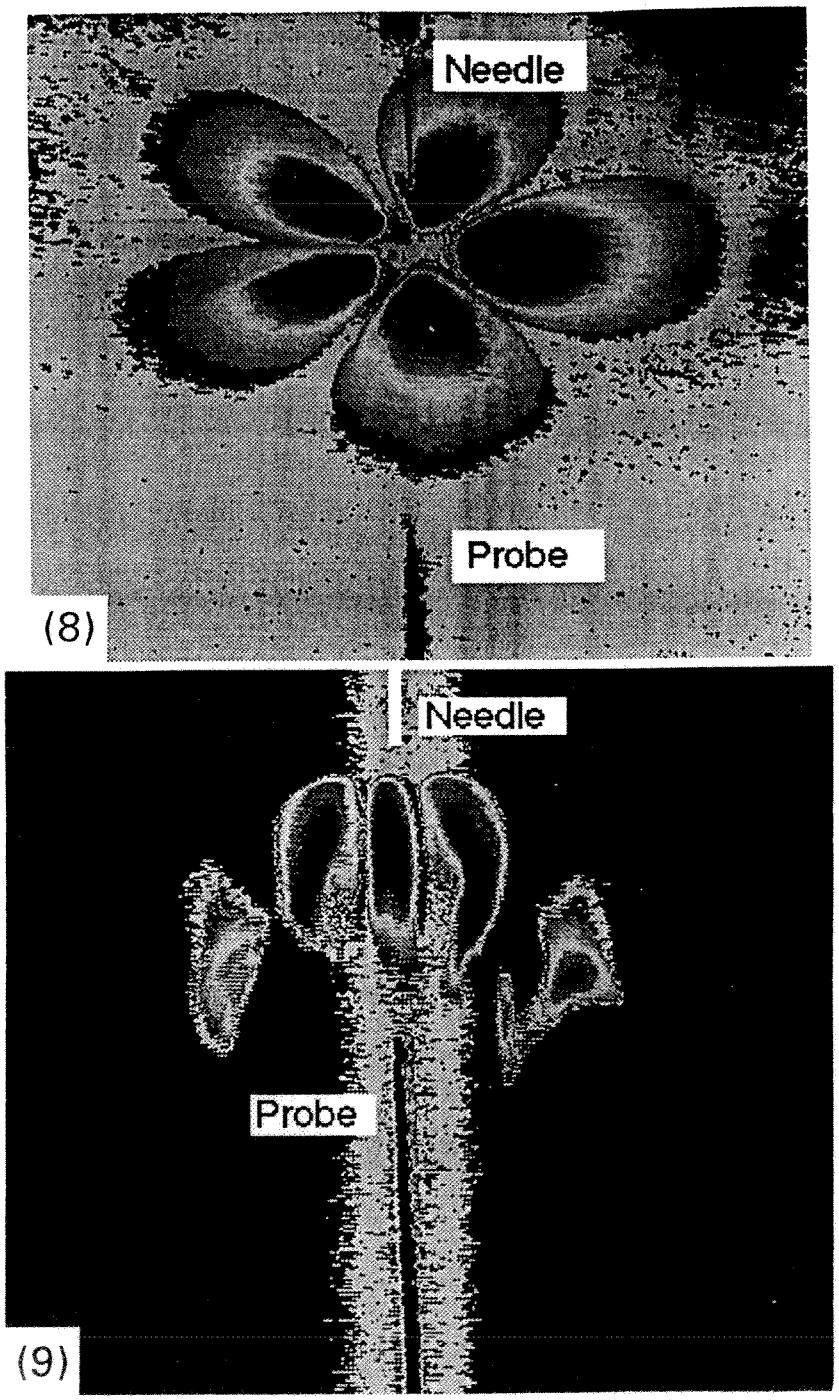

Fig. 8. Horizontal light-sheet visualization at 5 mm axial position of the EHD fine spray for the "on-axis" configuration at a spray charge density of 70 C m^{-3}. Each droplet "circulation cell" has an approximate 2 cm × 4 cm cross-sectional area.

Fig. 9. Vertical light-sheet visualization of the EHD fine spray for the "on-axis" configuration at a spray charge density of 70 C m^{-3}. The vertical distance between the needle's tip and probe's tip is 4 cm.

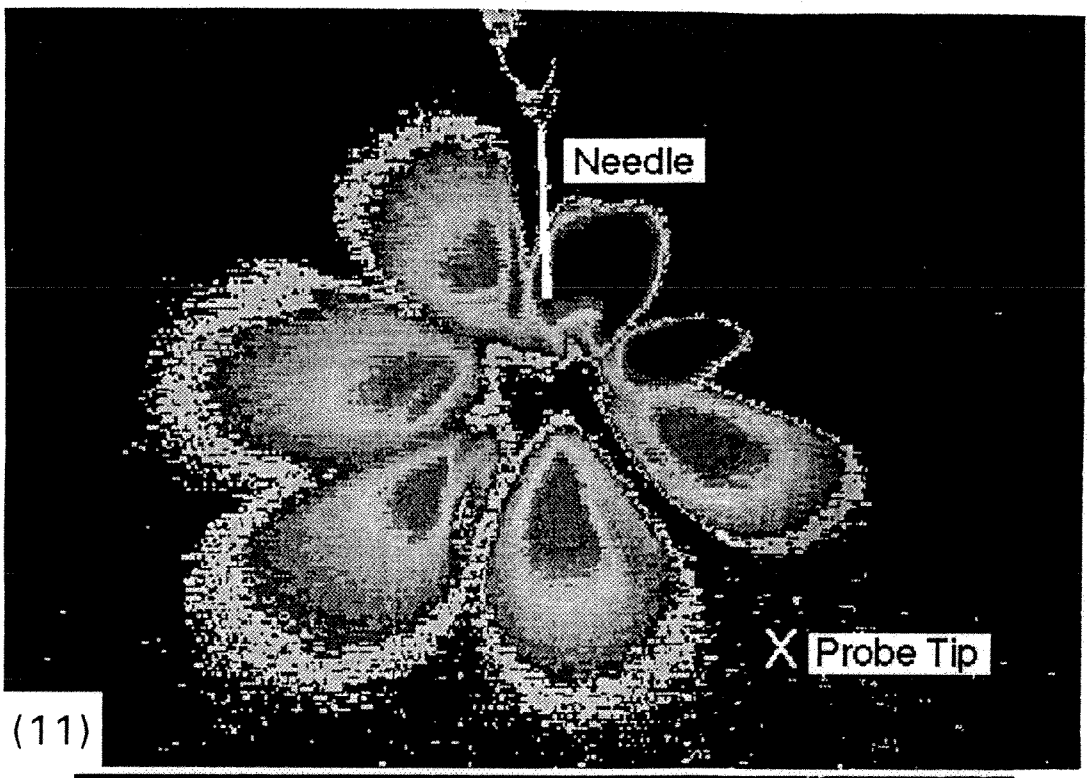

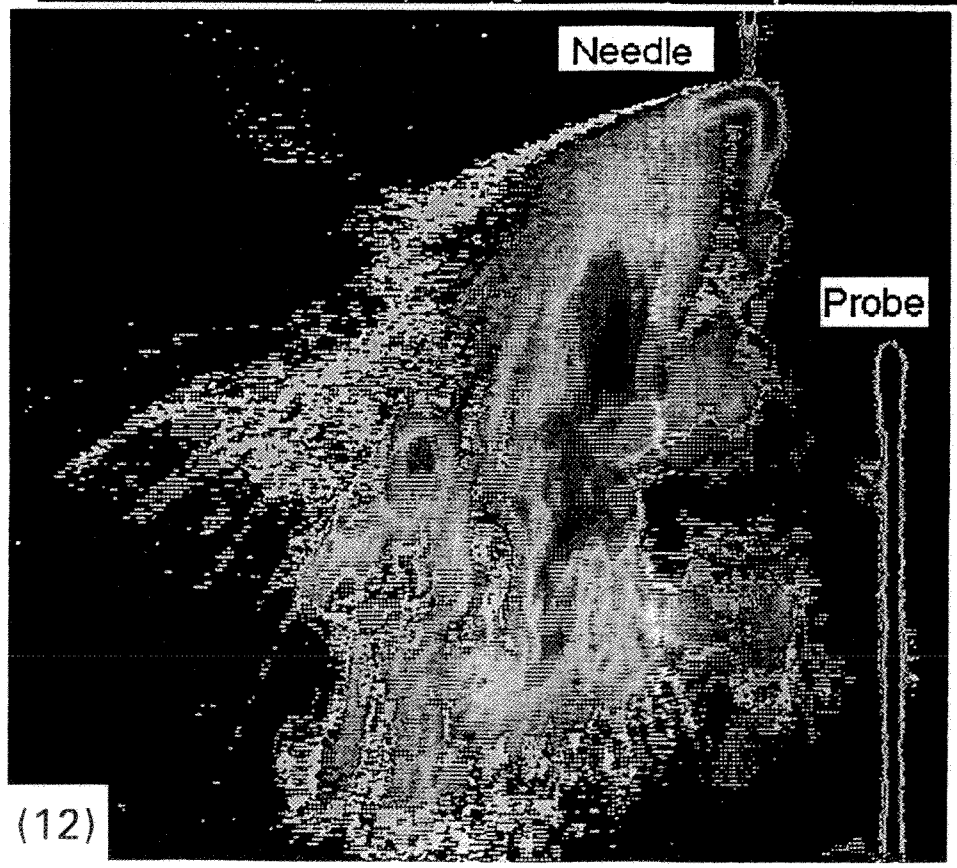

Fig. 11. Horizontal light-sheet visualization at 5 mm axial position of the EHD fine spray for the "off-axis" configuration at a spray charge density of 70 C m^{-3}. Each droplet "circulation cell" has an approximate 2 cm × 4 cm cross-sectional area.

Fig. 12. Vertical light-sheet visualization of the EHD fine spray for the "off-axis" configuration at a spray charge density of 70 C m^{-3}.

having equivalent dimensions. Each cell is observed to result from the breakup of an individual ligament and remains intact and does not mix with adjacent cells until far downstream. Far field visualizations reveal that the cells diffuse outwardly with increasing axial distance, but still retain isolated regions of high number concentration. A significant reduction in the lateral extent of the spray is evident in Fig. 9, as compared to the normal case (see Fig. 6).*

A "circulation cell" created in this configuration is the primary mechanism that promotes intra-spray mixing. These cells have a characteristically high velocity on the boundary and a low velocity inside the cell, as shown in the velocity vector diagram for the 20 μm diameter droplets in Fig. 10. Droplet diameter measurements indicate that larger droplet populations exist near the cell boundary, while the near-centerline locations are dominated by smaller droplets. This is a consequence of the high curvature of the electric field lines that are produced in this configuration. These populations are mixed convectively downstream of the "circulation cell" where droplets from the boundary are forced radially inward and droplets from the centerline are forced radially outward. Low speeds are measured within the "circulation cell" and regions of high speeds surrounding the cell. Beyond the influence of the "circulation cells", at approximately one-half of the distance toward the plate, the measured velocities and speeds exhibit the same trends as seen in the normal case.

The "off-axis" configuration

The horizontal light-sheet visualizations for this configuration revealed distinct "circulation cells", similar to those observed in the on-axis configuration. However, as shown in Fig. 11, the asymmetry of this configuration leads to a disruption of the cells nearest the probe tip, which consequently produces significant downstream interaction. At a downstream location where symmetrical structures still persisted in the on-axis case, the off-axis case shows highly distorted structures and significant interaction between adjacent structures.

The vertical light-sheet visualization, as displayed in Fig. 12, shows that the initial asymmetry of the configuration dramatically influences the downstream motion of the droplets. The "circulation cells" that were evident in the on-axis configuration are now smaller and more numerous. The droplet convergence–repulsion cycles responsible for the structure interaction in the on-axis case, have a higher frequency (~ 5 Hz). The exact cause of this increase in frequency is not known. The "circulation cells" do not show the extent of radial displacement with respect to the needle as was seen in the on-axis configuration because of the initial radial displacement of the probe relative to the needle's axis. The droplets, however, still exhibit a region of acceleration around the "circulation cell". This yields smaller "circulation cells", which allows for a higher droplet convergence and a higher cell convergence–repulsion frequency.

Additional visualizations reveal not only that there is convection in the form of large-scale cellular motion, but also that there is diffusion in the form of cell expansion. The vertical visualization provides the most compelling evidence for droplet mixing, showing that droplets from one location do interact with droplets from previously inaccessible locations. Thus, this configuration forces more rapid convective transport and a correspondingly higher degree of intra-spray droplet mixing.

Lateral expansion of the spray

Modification of the local electric field within the spray also significantly affects the lateral extent of the spray. This can be demonstrated readily by examining the outer boundary of the spray as determined from vertical laser light-sheet visualizations. As displayed in Fig. 13, there is a substantial reduction (of up to $\sim 600\%$!) in the spray's lateral extent for both

* Note that Figs 6 and 9 do not have the same scale.

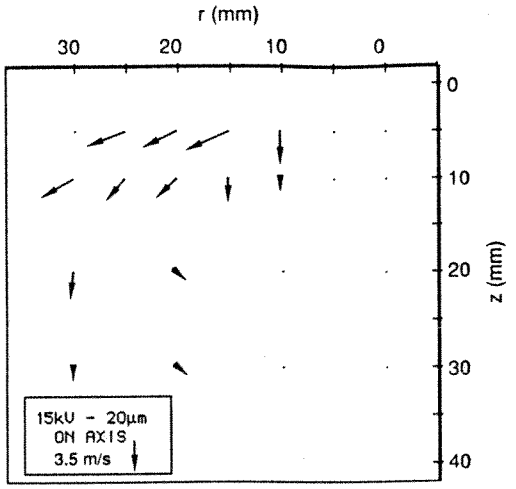

Fig. 10. Velocity vector diagram of 20 μm-diameter droplets in the EHD fine spray for the "on-axis" configuration at a spray charge density of 70 C m^{-3}. Note the difference in scale compared to Fig. 7. The tips of the needle and of the probe are located at the coordinates (0,0) and (0,40 mm), respectively.

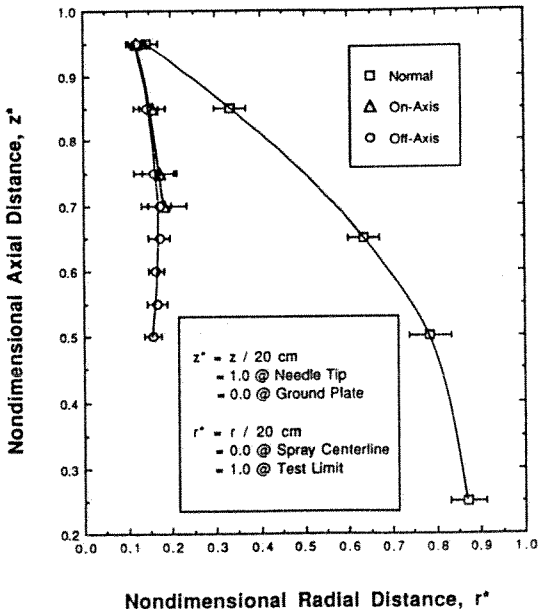

Fig. 13. Lateral extent of the EHD spray for "normal", "on-axis" and "off-axis" configurations.

modified-field cases as compared to the normal case. This reduction results directly from increased droplet convergence towards the probe's tip, which effectively limits the inherent radial expansion of the spray.

CONCLUSIONS

Droplets with similar levels of electrical charge can be mixed between and within EHD fine sprays despite their inherent tendency to repel one another. Mixing can be accomplished in several ways. In the case of two interacting EHD fine sprays, inter-spray droplet mixing occurs within certain regions of the combined spray. Experimental results illustrate that either increasing the spray charge density or decreasing the spacing between the sprays acts to promote the convergence of the two sprays, thereby enhancing inter-spray droplet mixing and the evolution toward a spatially uniform combined spray. In the case of a single EHD

fine spray, experiments reveal that spray expansion can be inhibited and large-scale droplet convection induced by introducing a small, electrically grounded surface within the spray, thus enhancing intra-spray droplet mixing.

These studies collectively support that the mixing of droplets with similar levels of electrical charge can be accomplished in simple ways. Such approaches may be desirable in practical applications where electrically charged liquid droplets need to be mixed homogeneously within confined spaces.

REFERENCES

Bachalo, W. D. and Houser, M. J. (1984) Phase Doppler spray analyzer for simultaneous measurement of droplet size and velocity distributions. *Optical Engng* **23**, 583–590.

Dunn, P. F. and Snarski, S. R. (1991) Velocity component and diameter distribution characteristics of droplets within two interacting electrohydrodynamic sprays. *Phys. Fluids* **3**, 494.

Dunn, P. F. and Snarski, S. R. (1992) Droplet diameter, flux, and total current measurements in an electrohydrodynamic spray. *J. appl. Phys.* **71**, 80–84.

Grace, J. M. (1993) Droplet motion and control in an electrohydrodynamic fine spray. Ph.D. Dissertation, University of Notre Dame, Notre Dame, IN.

Grace, J. M. and Dunn, P. F. (1992) Enhanced droplet mixing in an electrohydrodynamic spray. *Proceedings of the 5th Annual Conference on Liquid Atomization and Spray Systems*, pp. 220–224. San Ramon, CA.

Holve, D. J. and Annen, K. D. (1984) Optical particle counting, sizing, and velocimetry using intensity deconvolution. *Optical Engng* **23**, 591–603.

Nauman, E. B. and Buffham, B. A. (1983) *Mixing in Continuous Flow Systems*. Wiley, New York.

Ottino, J. M. (1989) *The Kinematics of Mixing: Stretching, Chaos and Transport*. Cambridge University Press, Cambridge.

Snarski, S. R. (1988) The interaction of electrohydrodynamically generated liquid droplets. M.S. Thesis, University of Notre Dame, Notre Dame, IN.

Snarski, S. R. and Dunn, P. F. (1991) Experiments characterizing the interaction between two sprays of electrically charged liquid droplets. *Experiments in Fluids* **11**, 268–278.

Vonnegut, B. and Neubauer, R. L. (1952) Production of monodisperse liquid particles by electrical atomization. *J. Colloid Sci.* **7**, 616–622.